Carbohydrate Polymers 85 (2011) 149–156

Contents lists available at ScienceDirect

Carbohydrate Polymers

journal homepage: www.elsevier.com/locate/carbpol

Fabrication and cellular compatibility of aligned chitosan–PCL fibers for nerve tissue regeneration

Ashleigh Cooper, Narayan Bhattarai [1], Miqin Zhang *

Department of Materials Science and Engineering, University of Washington, 302L Roberts Hall, Seattle, WA 98195, USA

ARTICLE INFO

Article history:
Received 8 August 2010
Received in revised form 28 January 2011
Accepted 3 February 2011
Available online 2 March 2011

Keywords:
Chitosan
Aligned nanofibers
Tissue engineering
Nerve

ABSTRACT

The ability to produce aligned sub-micron fibers may open new avenues for the development of scaffolds for application in tissue engineering and regenerative medicine. An area of particular interest is functional restoration of damaged or diseased nerves where the aligned fibers serve to support cell adhesion and proliferation, and guide neurite outgrowth in the direction of fiber orientation. In this study, we developed an aligned chitosan–polycaprolactone (chitosan–PCL) fibrous scaffold and investigated how the fiber alignment influenced nerve cell organization and function in comparison with randomly oriented fibrous scaffolds and cast films of the same material. Schwann cells (SCs) were shown to attach and proliferate on all the substrates regardless of their topography, demonstrating the cellular compatibility of the chitosan–PCL material. SCs grown on the aligned chitosan–PCL fibers exhibited a bipolar morphology that oriented along the fiber alignment direction, while those on the films and randomly oriented fibers had a multipolar morphology. Similarly, the chitosan–PCL material supported neuron-like PC-12 cell adhesion, and the aligned fibers regulated the growth of PC-12 cells along the fiber orientation. Additionally, PC-12 cells cultured on the aligned fibers exhibited enhanced unidirectional neurite extension along fiber orientation and significantly higher β-tubulin gene expression than those grown on chitosan–PCL films and randomly oriented fibers. Our investigation suggested that the aligned chitosan–PCL fibers can serve as a suitable scaffold for improved nerve tissue reconstruction.

1. Introduction

Peripheral nerve injury is relatively common, often resulting from tumor resection, reconstructive surgery or trauma. As of now, there is no satisfactory solution for repairing long peripheral nerve gaps. Autografting is unsatisfactory on functional recovery and suffers from site morbidity and multiple surgeries. The use of bioengineered scaffolds as synthetic nerve grafts has been identified as a promising approach, but existing scaffolds have not demonstrated the efficacy that is comparable to the performance of autografts (Cao, Liu, & Chew, 2009; Prabhakaran et al., 2008). This is largely due to the strict requirements for scaffolds used for nerve repair, unavailability of ideal scaffolding materials, and limited knowledge in the interaction of nerve cells with scaffolds. In addition to meeting general requirements for tissue engineering such as biocompatibility, high porosity and biodegradability, the scaffold material for nerve regeneration should have good pliability for suture and mechanical integrity during implantation to maintain an unimpeded pathway to support axon regeneration across large nerve defects, and provide contact guidance for cell migration and axon outgrowth along the defect gap for enhanced nerve regeneration.

In recent years, fibrous materials have been extensively studied as promising scaffolding materials for nerve repair, due to their structural similarity to the extracellular matrix (ECM) proteins of native tissues that regulate cell behavior and unique mechanical properties such as high mechanical strength and pliability. Various synthetic and natural polymer fibers with fiber diameters ranging from tens to hundreds of nanometers have been fabricated to meet special property requirements for nerve tissue regeneration. Synthetic polymers such as poly(lactic acid), polycaprolactone (PCL), and poly(D,L-lactide-co-glycolic acid) (PLGA) have been investigated as fibrous scaffolds due to their slow degradation required for nerve regeneration and good mechanical properties (Cao et al., 2009; Ghasemi-Mobarakeh, Prabhakaran, Morshed, Nasr-Esfahani, & Ramakrishna, 2008; Schnell et al., 2007). However, synthetic polymers are typically hydrophobic and lack cell-recognition sites for support of cell adhesion (Cao et al., 2009). Alternatively, natural polymers such as collagen and chitosan have shown good tissue compatibility and benign degradation products, but are mechanically weak and have a fast degradation rate. As a result, composite fibrous scaffolds of synthetic and natural polymers have been investigated to take the advantages of individual polymers for nerve

* Corresponding author. Tel.: +1 206 616 9356; fax: +1 206 543 3100.
E-mail address: mzhang@u.washington.edu (M. Zhang).
[1] Current address: Department of Bioengineering, North Carolina A&T University, Greensboro, NC 27411, USA.

0144-8617/$ – see front matter © 2011 Elsevier Ltd. All rights reserved.
doi:10.1016/j.carbpol.2011.02.008

regeneration (Ghasemi-Mobarakeh et al., 2008; Jiang, Lim, Mao, & Chew, 2009; Valmikinathan, Defroda, & Yu, 2009). For example, PCL-gelatin and -collagen randomly oriented fibrous substrates have been prepared with improved structural stability and biocompatibility compared to the individual polymers. However, many synthetic and natural polyblend fibers require chemical crosslinking to retain their structural integrity and improve mechanical strength (Choi, Lee, Christ, Atala, & Yoo, 2008; Kim et al., 2010), and the cytotoxicity of these crosslinking agents can be a challenge for biomedical applications due to increased toxicity.

We previously reported the design and fabrication of a nonwoven fibrous scaffold comprised of well-blended chitosan and poly(caprolactone) (PCL) with good mechanical and biological properties favorable for nerve regeneration (Bhattarai et al., 2009). Chitosan, a natural polymeric material, bears the proxy structure of glycosaminoglycan, a major component of the native ECM, which would provide a microenvironment with favorable physicochemical properties for cell adhesion and proliferation (Dang & Leong, 2006; Lee, Jeong, Kang, Lee, & Park, 2009). Commonly produced from shells of crustaceans (lobsters, crabs, and shrimps), chitosan has unlimited material sources, and unlike other natural polymers derived from costly mammalian proteins, chitosan with a high degree of deacetylation (>85%) evokes minimal foreign body response or fibrous encapsulation (Barbosa, Amaral, Águas, & Barbosa, 2010; Jayakumar, Prabaharan, Nair, & Tamura, 2010; Kim et al., 2008) which reduces the chance of immune rejection upon implantation. Produced without chemical crosslinking, the chitosan–PCL polyblend fibers exhibit enhanced mechanical properties under both wet and dry conditions compared to PLGA fibrous conduits and collagen, and enhanced cellular behavior (Bhattarai et al., 2009), and thus would serve as a improved substrate compared to other PCL–protein constructs.

Studies have shown that the fiber orientation influences cell adhesion, growth and modulates elongated cellular patterns that are typical of morphology found in native tissues (Murugan & Ramakrishna, 2007; Yao, O'Brien, Windebank, & Pandit, 2009). For nerve regeneration studies, aligned fibers of PCL (Chew, Mi, Hoke, & Leong, 2008), chitosan (Wang et al., 2009), PCL-gelatin (Ghasemi-Mobarakeh et al., 2008) and PCL-collagen (Schnell et al., 2007) have shown improved attachment and growth of nerve cells compared to random fibers.

In this study, we developed an aligned chitosan–PCL fibrous scaffold by electrospinning and investigated how the fiber alignment would influence cell adhesion, proliferation, and organization with Schwann cells (SC) and PC-12 cells. SCs were chosen in this study because they serve to support the attachment and growth of neurons wherein their alignment directs neurite outgrowth and promotes nerve regeneration (Sinis et al., 2005). Neuron-like PC-12 cells were used to examine the ability of the fibrous scaffold to support neurite extension necessary for nerve regeneration (Foley, Grunwald, Nealey, & Murphy, 2005). The cellular responses were assessed on chitosan–PCL with three different morphologies: aligned fibers, randomly oriented fibers, and cast films. Cell proliferation was quantified by AlamarBlue assays and cell morphology was examined by SEM. The ability of the aligned chitosan–PCL fibrous structure to support PC-12 cell differentiation was identified by neurite outgrowth and up-regulation of gene expression, assessed by immunocytochemical staining and real time PCR, respectively.

2. Materials and methods

2.1. Preparation of chitosan, PCL and chitosan–PCL solutions

Chitosan and PCL solutions were prepared separately, and mixed to create a stock solution of chitosan–PCL. Chitosan (85% deacetylated, Aldrich, St. Louis, MO) was dissolved in 7 wt% trifluoroacetic acid (TFA, Aldrich) and refluxed at 70 °C for 3 h, and PCL was dissolved in 2,2,2-trifluoroethanol (TFE, Aldrich, 12 wt%). Immediately prior to electrospinning, a chitosan–PCL solution was produced by mixing chitosan and PCL solutions at a ratio of 40:60, resulting in a final chitosan and PCL weight ratio of 25:75. This ratio was experimentally determined to produce fibers with a narrow size distribution and good stability in aqueous media (Bhattarai et al., 2009). For the chitosan electrospinning solution, 7 wt% chitosan was diluted with 10% methylene chloride. For the PCL electrospinning solution, a 10% PCL solution in TFE was prepared. To produce chitosan–PCL films as control samples, the chitosan and PCL solutions were diluted to 1 and 1.7 wt% in their corresponding solvents to produce a solution that was appropriate for spin-coating. Prior to spin coating, a chitosan–PCL solution was prepared by mixing the diluted chitosan and PCL solutions at a ratio of 40:60 to maintain the same polymer ratio as used for electrospinning.

2.2. Preparation of electrospun fibers and chitosan–PCL films

To produce electrospun fibers, approximately 2 mL of the solution was placed in a 3 mL syringe and a 200 μL syringe tip was fitted. The syringe tip was placed approximately 20 cm from a collector, oriented −25° from the horizontal, and a 22 kV voltage supply was used to charge the solution. The solution was spun towards either a rotating grounded drum (200 rpm) or a pair of grounded parallel electrodes (separation distance ~4 cm), for collecting randomly oriented and aligned fibers, respectively, and the fibers were allowed to dry overnight in a chemical hood. The collected fiber samples were attached to a 10 mm diameter coverslip using biocompatible poly L-lactide (Boehringer, Ingelheim, Germany) dissolved in hexafluoroisopropanol (Aldrich) at 3.5 wt%. Chitosan–PCL films (as a two-dimensional control) were prepared by spin-coating the dilute chitosan–PCL solution on a round, 10 mm coverslip. Due to the acidic nature of the solvents used, residual acid may have remained in the chitosan–PCL. Thus, all the fibers and films were neutralized with 14% ammonium hydroxide for 5 min, followed by rinsing with copious amounts of DI water. Samples were sterilized with 70% ethanol prior to cell seeding. As TFE is soluble in water, the amount of residual solvent was expected to be minimal.

2.3. Thermogravimetric analysis (TG, DTG)

Thermogravimetric (TG) analysis and differential thermogravimetric (DTG) analysis were performed with a Perkin Elmer TGA 7 (Waltham, MA). All analyses were performed with a ~10 mg sample placed in an aluminum pan under a nitrogen atmosphere at 50–750 °C. The experiments were run at a scanning rate of 10 °C/min. A weight loss profile with temperature including the maximum thermal decomposition temperature (T_m) was obtained using Pyris V. 06 software. The chitosan–PCL composition was calculated based on the assumption that the melting peak of pure PCL corresponded to 100% of the material.

2.4. Fiber and film characterization

To characterize the bonding of the PCL and chitosan, polarized FTIR spectra of 200 scans at 4 cm^{-1} resolution were obtained using a Nicolet 5DX spectrometer equipped with a DTGS detector and a solid transmission sample compartment. To characterize fiber morphology, the samples were sputter coated with gold for 30 s at 18 mA and imaged with a JEOL 7000F SEM (JEOL Ltd., Japan) at an accelerating voltage of 5–10 kV. The diameter of the electrospun fibers was determined by measuring one hundred individual fibers with ImageJ 1.42q software (NIH, Bethesda, Maryland, USA). ImageJ was used to assess the fiber alignment by superimposing a grid on

an SEM image and measuring the angle between the fiber and vertical grid lines. The mean angle of the fibers was subtracted from the individual fibers to normalize the fiber alignment to a horizontal reference. A fiber angle histogram within a range of ±90° was plotted and the percent of aligned fibers was calculated as the number of fibers in ±20°.

To evaluate the structural stability and integrity, the fibers were subjected to incubation at 37 °C for up to 30 days in lysozyme-rich PBS. After incubation, the fibers were rinsed with DI water, frozen and lyophilized to completely dry the samples without changing the structure of the fibers. The resulting samples were then imaged with SEM and TEM to determine changes in morphology and composition phase.

The mechanical properties of the randomly oriented and aligned chitosan–PCL fibers were measured with an Instron 5543 mechanical tester (Instron Corp, Norwood, MA) with a 10 N load cell at a strain rate of 10 mm/min. The thickness of the specimen was measured at five different points with an optical microscope and the values were averaged. Five samples of each condition were strained to fracture, and the tensile modulus, yield strength, tensile strength and percent elongation at break were averaged.

2.5. Cell culture

Schwann cells (SCs, ATTC, RT4-D6P2T, Manassas, VA) were stably transfected with p-EGFP-N1 using the Effectene Transfection Reagent kit (Qiagen, Valencia, CA) and maintained in Dulbecco's modified Eagle's medium (DMEM, Invitrogen, Carlsbad, CA) with 10% fetal bovine serum (FBS, Invitrogen), 1% penicillin–streptomycin (Invitrogen) and 1 mg/mL G418 sulfate (Fisher Scientific, Pittsburgh, PA). SCs were cultured on samples at a density of 12,500 cells/well in 24-well culture plates for three days. PC-12 cells (ATTC) were cultured on samples at a density of 50,000 cells/well containing F12K media (Invitrogen) with 2% horse serum (Invitrogen), 1% penicillin–streptomycin and 50 ng/mL nerve growth factor (NGF, 2.5 s mouse, Abcam). The samples were cultured with PC-12 cells for seven days with media change every two days.

2.6. Schwann cell viability and proliferation

A CytoTox 96 Nonradioactive assay (Promega, Madison, WA) was used to assess the cytotoxicity of chitosan–PCL samples. The colorimetric assay measures lactose dehydrogenase (LDH) in the supernatant, which is released upon cell lysis. Samples were cultured with SCs for three days and cell culture plates without chitosan–PCL were used as control. The media was sampled and assayed 1, 2, and 3 days after seeding following the manufacturer's protocol, and the absorbance was measured at 490 nm.

The alamarBlue colorimetric assay (Invitrogen) was used to analyze proliferation of the SCs on chitosan–PCL samples and on a cell culture plate. After 1, 2, and 3 days of culture, the samples were transferred to new well plates, washed twice with PBS (Invitrogen), and incubated with 10 vol% alamarBlue in serum-free DMEM with 10% FBS for two hours. 300 μL of the assay solution was transferred to an opaque 96-well culture plate for fluorescent measurements at 600 nm using a spectrophotometer (SpectraMax M2e, Molecular Devices). The relative fluorescent units were converted to cell number using a calibration curve produced by measuring the fluorescence of known cell numbers. Reported cell numbers were normalized to the culture area (cm^2) to account for the larger growth area of the well-plate (1.91 cm^2) as compared to the round coverslips (1.13 cm^2) used for the chitosan–PCL samples.

2.7. Schwann cell morphology analysis

Microscopy analysis was performed to examine the SC attachment to the chitosan–PCL samples. For SEM analysis of SC attachment, samples were removed from media after three days of culture, rinsed with PBS, and fixed with Karnovsky's fixative overnight. After fixing, samples were briefly rinsed with DI water and dehydrated with sequential rinses with 50, 75 and 100% ethanol for 15 min each. Samples were sputter-coated with Au/Pd for 30 s at 18 mA and imaged with SEM. For fluorescent microscopy studies, SCs were cultured for three days, rinsed briefly with PBS to remove debris, and fixed in 4% methanol-free formaldehyde (Aldrich) for 15 min. The samples were rinsed in PBS and mounted to a coverslip with Prolong Gold Antifade reagent with DAPI (Invitrogen). The samples were cured overnight at room temperature and imaged with a confocal fluorescent microscope (Zeiss Meta 510 Confocal Microscope, Germany).

2.8. Immunocytochemistry

For immunocytochemistry studies of the PC-12 interactions with chitosan–PCL, the samples were fixed in 4% methanol-free formaldehyde in PBS for 15 min. The samples were then washed in ice-cold PBS, and the cell membrane was permeabilized with 0.25% Triton X-100 (Aldrich) in PBS for 10 min. Following permeabilization, the samples were incubated with 10% rabbit serum (Abcam, Cambridge, MA) in PBS for 30 min to block non-specific protein binding, and with rabbit monoclonal, LANGF receptor antibody (MC-192, Abcam) at a 1:500 dilution in PBS with Triton X-100 overnight at 4 °C. The samples were then incubated in a 1:500 dilution of FITC conjugated rabbit secondary antibody (Abcam) in PBS for one hour. All incubation steps, except the overnight incubation, were performed at room temperature, and the samples were rinsed three times with PBS between each step. The samples were mounted to a coverslip with Prolong Gold Antifade reagent with DAPI (Invitrogen). The samples were cured overnight and imaged with a confocal fluorescent microscope.

2.9. Quantitative RT-PCR analysis of PC-12 cells

PC-12 cells were cultured on samples for seven days, and the gene expression of GAPDH, β-tubulin and neurofilament-200 (NF-200) were analyzed. GAPDH was used as a housekeeping gene, and β-tubulin and NF-200 were used as indicators to the formation of neurites. To extract the RNA, the samples were rinsed briefly in PBS to remove serum, covered with RNAlater (Qiagen, Valencia, CA), and frozen at −80 °C. Cellular mRNA was collected with a Qiagen RNeasy Plus kit, the lysis buffer was pipetted firmly over the substrates to detach cells, and the Qiagen protocol was followed. mRNA was concentrated in a 30 μl volume, and mRNA reverse transcription was performed with a Qiagen Omniscript RT kit. DNA transcripts were then probed using Qiagen Quantitect SYBR Green. Thermocycling was performed with a BioRad CFX96 real-time detection system (Bio-Rad, Hercules, CA) at the following conditions: 95 °C for 15 min, 45 cycles of denaturation (15 s, 94 °C), annealing (30 s, 55 °C), and extension (30 s, 72 °C). The relative expression of each gene was compared to the expression of GAPDH to eliminate the effect of cell population, and the results were normalized to the gene expression of cells on the chitosan–PCL films.

2.10. Statistical analysis

Statistical analyses of the cytotoxicity, cell proliferation and PCR study were performed using one-way analysis of variance (ANOVA). *P* values less than 0.05 were considered statistically sig-

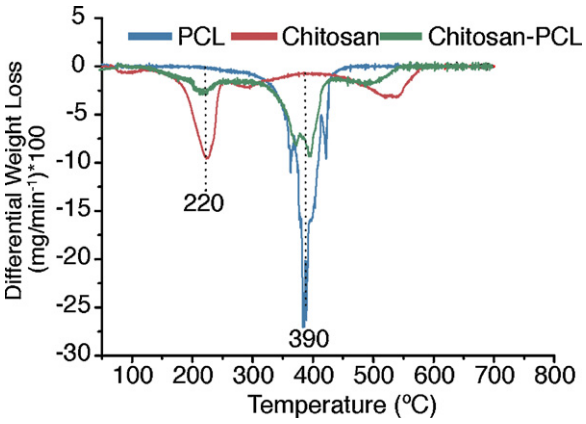

Fig. 1. DTG thermograms of chitosan, PCL, and chitosan–PCL fibers.

nificant, and differences between samples within the groups were evaluated using a Student's *t*-test.

3. Results and discussion

3.1. Physicochemical properties of chitosan–PCL fibers

A tissue-engineering scaffold that blends natural and synthetic materials must demonstrate physical homogeneity and miscibility to ensure the structural stability in aqueous media, which is of vital importance for biomedical applications, and preservation of the biocompatible properties of the natural material. An important advantage of chitosan is its hydrophilic nature and presence of free amino groups that have been shown to contribute to nerve cell attachment and extension (Chatelet, Damour, & Domard, 2001; Freier, Montenegro, Shan Koh, & Shoichet, 2005). However, due to the weak structural integrity and susceptibility to swelling in aqueous environments, chitosan was incorporated with PCL to produce a mechanically stable material.

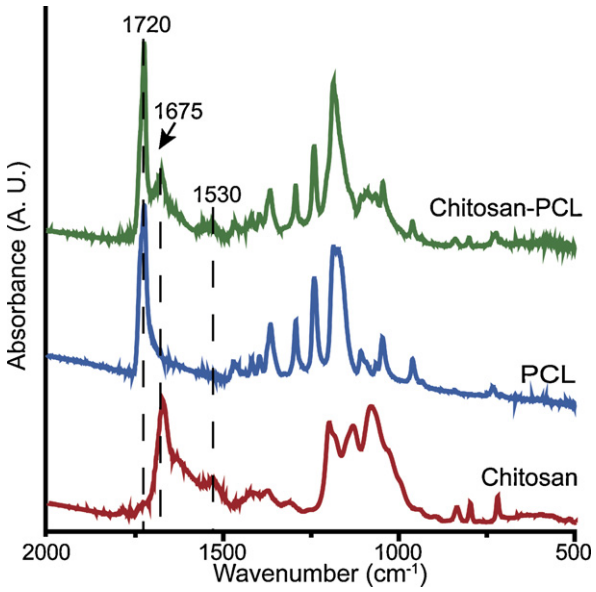

Fig. 2. FTIR characterization of PCL, chitosan and chitosan–fibers prepared by electrospinning. The spectra were averaged from 200 scans with a 4 cm^{-1} resolution.

TG/DTG analysis was performed to estimate thermal stability and the composition of individual polymers in the chitosan–PCL fibers (Fig. 1). Characteristic thermal degradation peaks of component polymers in the blended chitosan–PCL fibers were identified by comparing with the thermal degradation behaviors of chitosan and PCL fibers. Furthermore, the TG/DTG analysis also assessed the susceptibility of PCL to hydrolytic degradation by the trifluoroacetic acid during the electrospinning process. As shown in Fig. 1, a slight mass loss in chitosan fibers was observed at ~100 °C, which is related to the loss of bonded water in chitosan that had not been completely removed by the ambient drying process. The weight loss of the chitosan–PCL fiber at the same temperature was

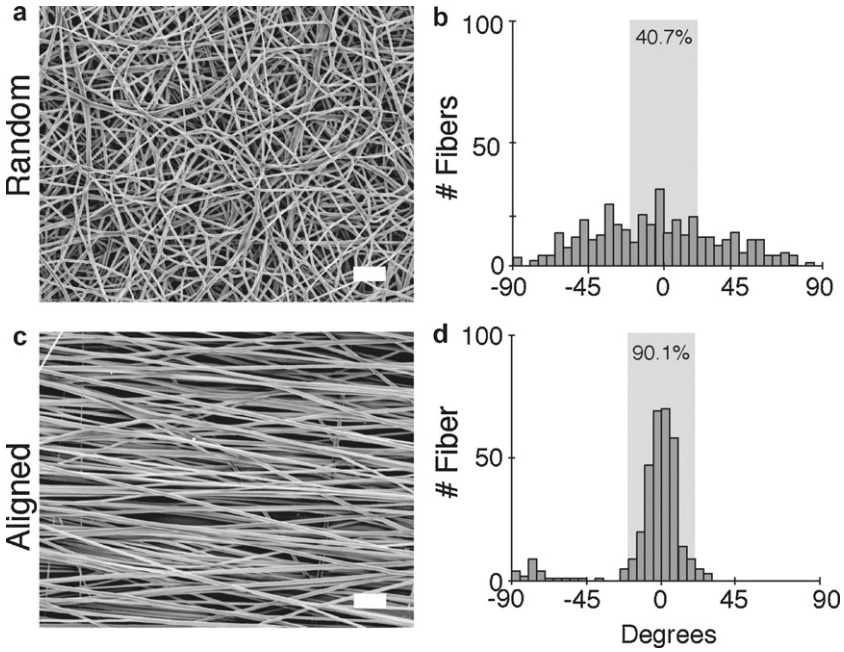

Fig. 3. Morphology and the degree of alignment of the chitosan–PCL fibers. SEM images and histograms illustrating the percentage of alignment (±20°) of (a, b) random and (c, d) aligned chitosan–PCL fibers. Scale bar indicates 5 μm.

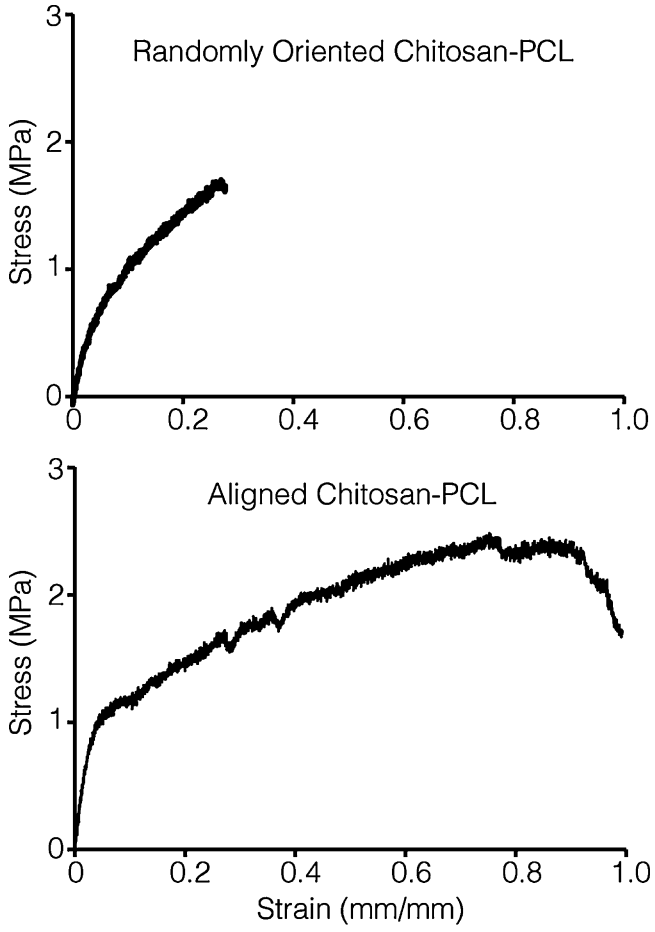

	Modulus (MPa)	YS (MPa)
Random	12.35 ± 1.38	0.68 ± 0.065
Aligned	22.41 ± 1.11	0.94 ± 0.01

	TS (MPa)	%Break at Elong.
Random	1.78 ± 0.25	31.13 ± 7.5
Aligned	2.64 ± 0.48	84.45 ±7.0

Fig. 4. Stress–strain curves of randomly oriented and aligned chitosan–PCL fibrous matrices tested at a strain rate of 10 mm/min. The mechanical properties are averaged from five individual tests. Also shown are the mechanical moduli and yield strength.

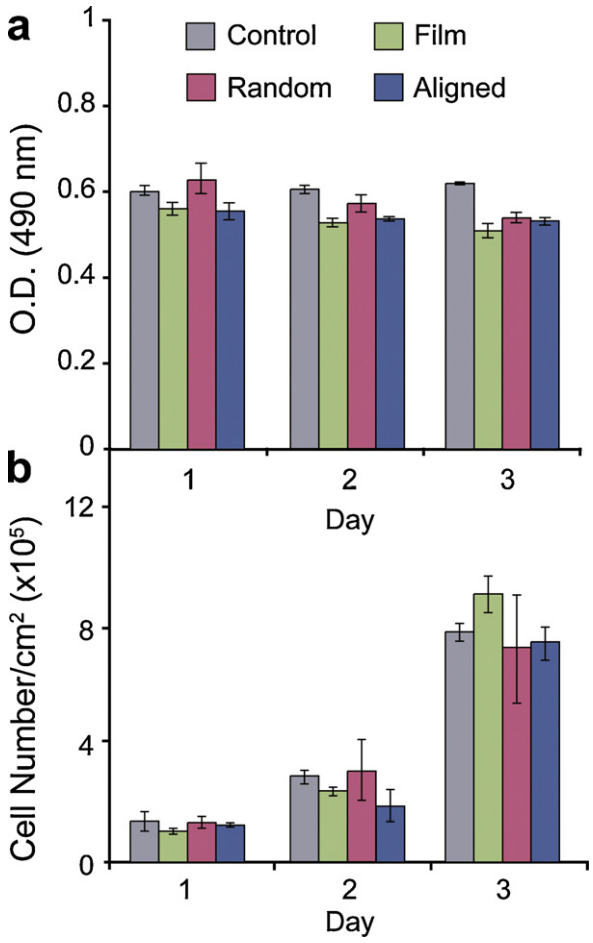

Fig. 5. Schwann cell interactions with chitosan–PCL. (a) Cytotoxicity of the materials measured in terms of LDH levels and (b) Schwann cell proliferation on control well-plates (control), chitosan–PCL films, randomly oriented and aligned chitosan–PCL fibers after three days of cell culture.

minimal. This suggests that the blend fibers contain much less moisture, which can be attributed to the presence of hydrophobic PCL and its intermolecular interaction with chitosan. At a maximum weight loss temperature of chitosan, $T_{max\text{-}chitosan}$, ~220 °C, both chitosan and chitosan–PCL samples showed weight loss due to thermal decomposition of the chitosan polysaccharide. However, the chitosan–PCL fibers have significantly lower mass loss than the chitosan fibers due to the presence of PCL. The thermoxidative degradation of PCL occurred at $T_{max\text{-}PCL}$ of ~390 °C. The chitosan–PCL fibers also had a T_{max}-chitosan–PCL at ~390 °C, but exhibited a depressed weight loss peak, due to the presence of chitosan that suppressed PCL crystallinity. These results indicate similar thermal stability of the PCL both in the chitosan–PCL and PCL fibers, illustrating that degradation of PCL did not occur during electrospinning with TFA. The distinct single step weight loss peak of PCL at 390 °C was used as a reference to estimate the percentage of PCL in the chitosan–PCL fibers. Considering the area of the peak at 390 °C was 100% weight loss of the PCL sample, the weight percentage of PCL in the chitosan–PCL fibers was estimated to be approximately 58 ± 4%, consistent with the original composition of chitosan and PCL. This result indicates that chitosan–PCL is thermally stable, and no loss or degradation of the chitosan and PCL occurred during the electrospinning process.

The bonding between PCL and chitosan in chitosan–PCL fibers was characterized by FTIR (Fig. 2). The spectrum of chitosan fibers showed a basic adsorption band of carboxylate ions at the 1400–1790 cm^{-1} region, with a maximum at 1675 cm^{-1} that overlapped the bands of amide and amino groups. The strong absorption band of PCL at 1720 cm^{-1} corresponds to the carbonyl groups. The characteristic absorption bands of the chitosan–PCL fiber were observed at 1675 and 1530 cm^{-1}, corresponding to the stretching of amide and protonated amine groups resulted from residual TFA in the electrospinning solution (Sangsanoh & Supaphol, 2006). This result indicates that representative amine and amino groups remained in the chitosan–PCL fibers. No additional peaks except the characteristic peaks of PCL and chitosan in the chitosan–PCL blend fibers were observed, indicating no covalent bonding between the polymers occurred (Elzein, 2004; Pawlak & Mucha, 2003). Possible physical interactions, such as the intermolecular hydrogen bonding between the carbonyl group of PCL and hydroxyl or ammonium ions of chitosan between the chitosan and PCL, remain. The synthesized chitosan–PCL fibers were incubated in phosphate buffered saline (PBS, pH 7.4) and cell culture media for two weeks and no swelling was observed, indicating the chitosan–PCL fibers are capable of retaining its structural integrity in an aqueous environment.

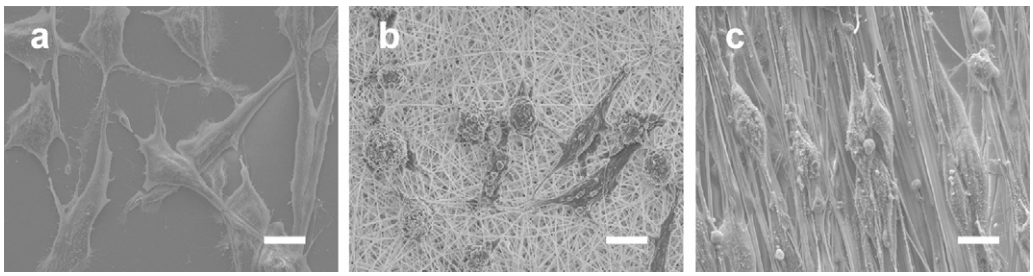

Fig. 6. SEM images of SCs (a) chitosan–PCL films, (b) randomly oriented, and (c) aligned chitosan–PCL fibers after three days of cell culture. Scale bars represent 10 μm.

3.2. Morphology and mechanical properties of chitosan–PCL fibers

The morphology of aligned and randomly oriented fibers was examined with SEM. As shown in Fig. 3a and c, randomly oriented and uniaxially aligned fibers had mean diameters of 405.0 ± 59.8 and 408.2 ± 76.6 nm, respectively. The degree of fiber alignment was evaluated as the percentage of fibers oriented ±20° from the horizontal, and the fiber alignment was 40.7% and 90.1% for the randomly oriented and aligned chitosan–PCL fibers, respectively (Fig. 3b and d). Although the random fibers had 40.7% alignment, the broad distribution of fiber angles with respect to a horizontal indicates a random orientation. Alternatively, the aligned fibers displayed a narrow distribution of fiber orientation.

Ideally, a nerve guide should have a Young's modulus approaching that of nerve tissues to resist in vivo physiological loading during nerve regeneration and provide sufficient strength and flexibility to be implanted and sutured during implantation (Gu, Ding, & Liu, 2010). It is generally accepted that Young's modulus of peripheral nerves (for example, a rabbit tibial nerve) in the longitudinal direction is in the range of 0.50 MPa (Gu et al., 2010). As shown in Fig. 4, the mechanical properties of the randomly oriented and aligned chitosan–PCL fibers differed considerably. The tensile modulus, yield strength, tensile strength and percent elongation for the aligned fibers were all greater than those for the randomly oriented fibers. Notably, the aligned chitosan–PCL fibers exhibited better ductility, which is favorable for material handling.

3.3. Biological properties of chitosan–PCL fibers

To evaluate the influence of sample topography on SC cytotoxicity and cell proliferation, SCs were cultured for three days

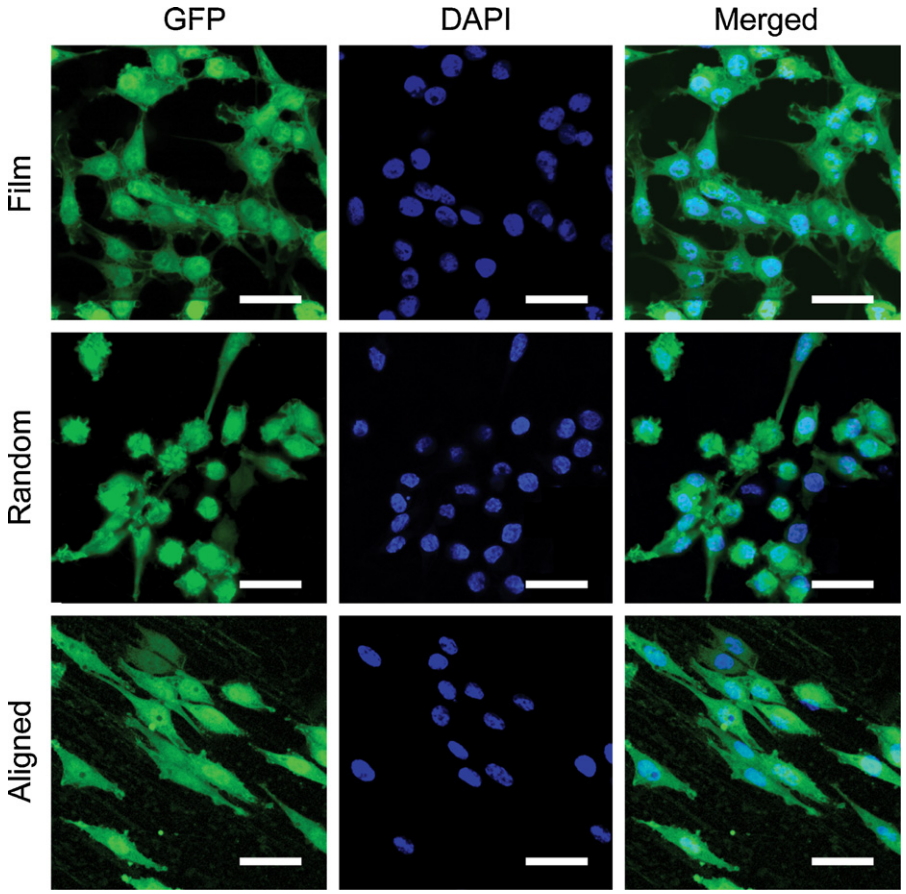

Fig. 7. Fluorescence images of Schwann cells on chitosan–PCL films, randomly oriented and aligned chitosan–PCL fibers after three days of cell culture. Cells were permanently transfected with p-EGFP-N1 (left column, green) and the nuclei were stained with DAPI (middle column, blue). The merged images of GFP and DAPI for each material are listed on the right column. Scale bars represent 20 μm. (For interpretation of the references to color in this figure legend, the reader is referred to the web version of the article.)

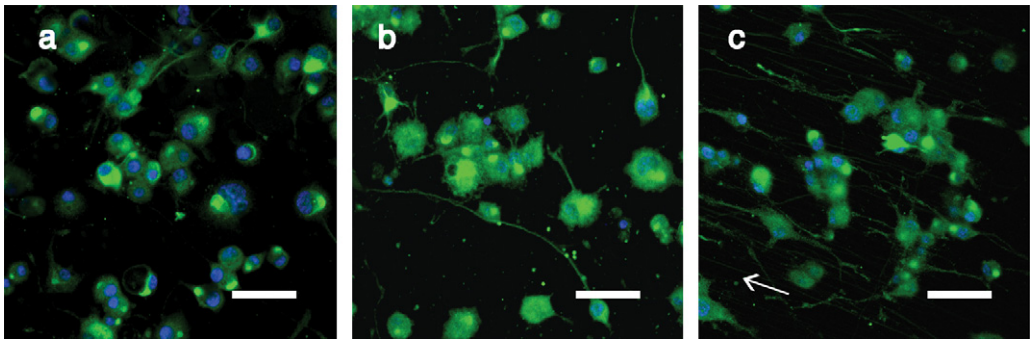

Fig. 8. Neuronal immunostaining of PC-12 cells on (a) chitosan–PCL films, (b) randomly oriented and (c) aligned chitosan–PCL fibers after seven days of cell culture. Cells were immunostained with ALDH1A1 antibody (green) and the nuclei were stained with DAPI (blue). The arrow in (c) indicates the direction of fiber alignment. Scale bars represent 10 μm. (For interpretation of the references to color in this figure legend, the reader is referred to the web version of the article.)

on chitosan–PCL films, random and aligned chitosan–PCL fibers, and cell culture plates (as control). The cell toxicity was tested by measuring the presence of lactose dehydrogenase (LDH), a cytoplasmic enzyme released from damaged cells. The cell number was measured with an alamarBlue assay and normalized to the sample surface area (cm^2). As shown in Fig. 5a, the LDH levels were approximately the same for all of the chitosan–PCL samples, regardless of topography, and were comparable to the level exhibited by SCs on the cell culture plates ($p > 0.05$). This result indicates that neither the chitosan–PCL material nor the material topography induced additional cell injury or death. As shown in Fig. 5b, SC proliferation on all of the material samples increased during the 3-day period and no significant difference in cell proliferation between the samples was identified, suggesting the material topography did not significantly ($p > 0.05$) influence cell proliferation under the conditions of this study.

Although the *in vitro* assays above illustrated the cellular biocompatibility of the chitosan–PCL, the direct cellular interactions with the material surface also plays an important role in tissue regeneration. For example, SC morphology and directionality is a key contributing factor to neuritogenesis (Chen, Yu, & Strickland, 2007; Más Estellés, Vidaurre, Meseguer Dueñas, & Castilla Cortázar, 2008). The influence of aligned chitosan–PCL fibers on regulating cell adhesion and spreading was investigated by incubating SCs on aligned chitosan–PCL fibers and comparing to SCs incubated on randomly oriented chitosan–PCL fibers and chitosan–PCL cast films. SCs cultured on the materials for three days were examined with SEM. As shown in Fig. 6, SCs grown on different chitosan–PCL samples exhibited substantially different morphologies. SCs on the films and randomly oriented fibers had multiple focal adhesions resulting in a multipolar morphology and flatter cell bodies. Alternatively, SCs on the aligned chitosan–PCL fibers appeared to interact with individual aligned fibers, exhibiting an extended, bipolar morphology that oriented along the fiber direction, which enhanced the cellular alignment. Confocal fluorescence images (Fig. 7) further illustrate the cellular morphology on the different samples. Although bipolar SCs were observed on the film and randomly oriented fibers, they were not aligned. The preferential alignment of SCs on the aligned fibers mimicked the early morphology necessary for the formation of Büngner bands to guide axonal regeneration (Más Estellés et al., 2008).

During nerve regeneration, axon growth and neurite extension occur in response to chemical and physical cues elicited from the local microenvironment. To evaluate the potential of aligned chitosan–PCL fibers to serve as a scaffold for nerve regeneration, neuron-like PC-12 cells were cultured on the chitosan–PCL samples for seven days, and analyzed for neurite extension using a neuronal marker and gene expression analysis. The neurite extension was observed by immunostaining PC-12 cells with antibody against

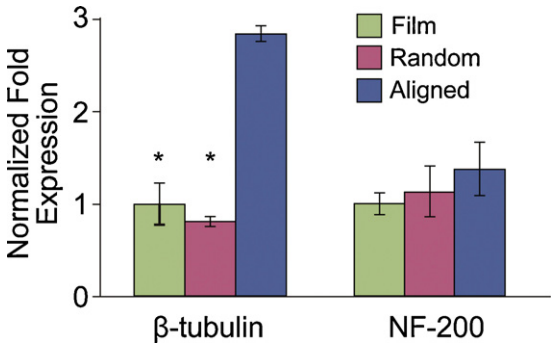

Fig. 9. β-Tubulin and neurofilament-200 (NF-200) gene expressions of PC-12 cells on chitosan–PCL films, randomly oriented and aligned chitosan–PCL fibers after seven days of cell culture. Asterisks denote significant difference ($p < 0.05$) compared to the aligned chitosan–PCL fibers.

nerve growth factor (NGF) receptor. As shown in Fig. 8, confocal fluorescence images of PC-12 cells showed a topographical response of cells to the aligned chitosan–PCL fibers, with neurite extension parallel to the fiber orientation (white arrow in Fig. 8c). PC-12 cells on the film and randomly oriented chitosan–PCL fibers exhibited shorter and randomly oriented neurites.

In addition to the morphological response to the material topography, the gene expressions of NF-200 and β-tubulin by PC-12 cells were monitored using real-time PCR. NF-200, a neurofilament is associated with cell differentiation and neurite growth (Lariviere & Julien, 2004). β-Tubulin, a dimer required for microtubule formation, is a major cytoskeletal component of neurite extension (He, Zhang, Yang, & Ding, 2009). As shown in Fig. 9, NF-200 expression was comparably expressed on all the samples, demonstrating that the chitosan–PCL scaffolds supported PC-12 differentiation. Notably, β-tubulin expression by PC-12 cells on the aligned chitosan–PCL fibers was three times greater than that on the randomly oriented fibers and films, illustrating that the aligned fibers enhanced neurite extension, consistent with cellular morphological analysis shown in Fig. 8c, where PC-12 neurites showed enhanced directionality along the fiber orientation.

4. Conclusions

Aligned chitosan–PCL fibers provide a favorable environment for nerve cell proliferation, and function. The highly aligned chitosan–PCL fibrous scaffolds were shown to direct SC attachment resulting in characteristic cell morphology necessary for nerve regeneration as compared to chitosan–PCL film and randomly oriented fibers. The fiber alignment enhanced the neurite extension and directionality of PC-12 cells, demonstrating the increased

cellular responses induced by oriented fiber topographies. PC-12 cells on the aligned fibers showed up-regulation of differentiation-specific gene expressions. Our study suggests that the chitosan–PCL fibers elicit chemical and topographical cues for the modulation of neuritogenesis and could serve as a potential scaffold for nerve regeneration. The developed chitosan–PCL fiber system could be potentially applied to other tissue types due to the demonstrated tissue compatibility of the constituent polymers.

Acknowledgments

This work is supported in part by GEMSEC, an NSF-MRSEC at the University of Washington (DMR-0520567). Ashleigh Cooper would like to acknowledge the Osberg and Bank of America Endowed Minority fellowships.

References

Barbosa, J., Amaral, I., Águas, A., & Barbosa, M. (2010). Evaluation of the effect of the degree of acetylation on the inflammatory response to 3D porous chitosan scaffolds. *Journal of Biomedical Materials Research*, *93*(1), 20–28.

Bhattarai, N., Li, Z., Gunn, J., Leung, M., Cooper, A., Edmondson, D., et al. (2009). Natural–synthetic polyblend nanofibers for biomedical applications. *Advanced Materials*, *21*, 2792–2797.

Cao, H., Liu, T., & Chew, S. Y. (2009). The application of nanofibrous scaffolds in neural tissue engineering. *Advanced Drug Delivery Reviews*, *61*(12), 1055–1064.

Chatelet, C., Damour, O., & Domard, A. (2001). Influence of the degree of acetylation on some biological properties of chitosan films. *Biomaterials*, *22*(3), 261–268.

Chen, Z. L., Yu, W. M., & Strickland, S. (2007). Peripheral regeneration. *Annual Review of Neuroscience*, *30*, 209–233.

Chew, S. Y., Mi, R., Hoke, A., & Leong, K. W. (2008). The effect of the alignment of electrospun fibrous scaffolds on Schwann cell maturation. *Biomaterials*, *29*(6), 653–661.

Choi, J. S., Lee, S. J., Christ, G. J., Atala, A., & Yoo, J. J. (2008). The influence of electrospun aligned poly(epsilon-caprolactone)/collagen nanofiber meshes on the formation of self-aligned skeletal muscle myotubes. *Biomaterials*, *29*(19), 2899–2906.

Dang, J. M., & Leong, K. W. (2006). Natural polymers for gene delivery and tissue engineering. *Advanced Drug Delivery Reviews*, *58*(4), 487–499.

Elzein, T. (2004). FTIR study of polycaprolactone chain organization at interfaces. *Journal of Colloid and Interface Science*, *273*(2), 381–387.

Foley, J. D., Grunwald, E. W., Nealey, P. F., & Murphy, C. J. (2005). Cooperative modulation of neuritogenesis by PC12 cells by topography and nerve growth factor. *Biomaterials*, *26*(17), 3639–3644.

Freier, T., Montenegro, R., Shan Koh, H., & Shoichet, M. (2005). Chitin-based tubes for tissue engineering in the nervous system. *Biomaterials*, *26*(22), 4624–4632.

Ghasemi-Mobarakeh, L., Prabhakaran, M. P., Morshed, M., Nasr-Esfahani, M. H., & Ramakrishna, S. (2008). Electrospun poly(epsilon-caprolactone)/gelatin nanofibrous scaffolds for nerve tissue engineering. *Biomaterials*, *29*(34), 4532–4539.

Gu, X., Ding, F. Y. Y., & Liu, J. (2010). Construction of tissue engineered nerve grafts and their application in peripheral nerve regeneration. *Progress in Neurobiology*, *93*(1), 204–230.

He, Q., Zhang, T., Yang, Y., & Ding, F. (2009). In vitro biocompatibility of chitosan-based materials to primary culture of hippocampal neurons. *Journal of Materials Science Materials in Medicine*, *20*(7), 1457–1466.

Jayakumar, R., Prabaharan, M., Nair, S. V., & Tamura, H. (2010). Novel chitin and chitosan nanofibers in biomedical applications. *Biotechnology Advances*, *28*(1), 142–150.

Jiang, X., Lim, S., Mao, H., & Chew, S. (2009). Current applications and future perspectives of artificial nerve conduits. *Experimental Neurology*.

Kim, I.-Y., Seo, S.-J., Moon, H.-S., Yoo, M.-K., Park, I.-Y., Kim, B.-C., et al. (2008). Chitosan and its derivatives for tissue engineering applications. *Biotechnology Advances*, *26*(1), 1–21.

Kim, M. S., Jun, I., Shin, Y. M., Jang, W., Kim, S. I., & Shin, H. (2010). The development of genipin-crosslinked poly(caprolactone) (PCL)/gelatin nanofibers for tissue engineering applications. *Macromolecular Bioscience*, *10*(1), 91–100.

Lariviere, R., & Julien, J. (2004). Functions of intermediate filaments in neuronal development and disease. *Development in Neurobiology*, *58*(1), 131–148.

Lee, K. Y., Jeong, L., Kang, Y. O., Lee, S. J., & Park, W. H. (2009). Electrospinning of polysaccharides for regenerative medicine. *Advanced Drug Delivery Reviews*, *61*(12), 1020–1032.

Más Estellés, J., Vidaurre, A., Meseguer Dueñas, J., & Castilla Cortázar, I. (2008). Physical characterization of polycaprolactone scaffolds. *Journal of Materials Science Materials in Medicine*, *19*(1), 189–195.

Murugan, R., & Ramakrishna, S. (2007). Design strategies of tissue engineering scaffolds with controlled fiber orientation. *Tissue Engineering*, *13*(8), 1845–1866.

Pawlak, A., & Mucha, M. (2003). Thermogravimetric and FTIR Studies of Chitosan Blends. *Thermochimica Acta*, *396*(2), 153–166.

Prabhakaran, M. P., Venugopal, J. R., Chyan, T. T., Hai, L. B., Chan, C. K., Lim, A. Y., et al. (2008). Electrospun biocomposite nanofibrous scaffolds for neural tissue engineering. *Tissue Engineering Part A*, *14*(11), 1787–1797.

Sangsanoh, P., & Supaphol, P. (2006). Stability improvement of electrospun chitosan nanofibrous membranes in neutral or weak basic aqueous solutions. *Biomacromolecules*, *7*(10), 2710–2714.

Schnell, E., Klinkhammer, K., Balzer, S., Brook, G., Klee, D., Dalton, P., et al. (2007). Guidance of glial cell migration and axonal growth on electrospun nanofibers of poly-epsilon-caprolactone and a collagen/poly-epsilon-caprolactone blend. *Biomaterials*, *28*(19), 3012–3025.

Sinis, N., Schaller, H. E., Schulte-Eversum, C., Schlosshauer, B., Doser, M., Dietz, K., et al. (2005). Nerve regeneration across a 2-cm gap in the rat median nerve using a resorbable nerve conduit filled with Schwann cells. *Journal of Neurosurgery*, *103*(6), 1067–1076.

Valmikinathan, C. M., Defroda, S., & Yu, X. (2009). Polycaprolactone and bovine serum albumin based nanofibers for controlled release of nerve growth factor. *Biomacromolecules*, *10*(5), 1084–1089.

Wang, W., Itoh, S., Konno, K., Kikkawa, T., Ichinose, S., Sakai, K., et al. (2009). Effects of Schwann cell alignment along the oriented electrospun chitosan nanofibers on nerve regeneration. *Journal of Biomedical Materials Research A*, *91*(4), 994–1005.

Yao, L., O'Brien, N., Windebank, A., & Pandit, A. (2009). Orienting neurite growth in electrospun fibrous neural conduits. *Journal of Biomedical Materials Research B Applied Biomaterials*, *90*(2), 483–491.